

Modelling of a gas turbine combustor using a network solver

J.J. Gouws*, R.M. Morris*[†] and J.A. Visser*

In this study, a one-dimensional empirical model was developed and integrated with a commercial network solver to predict flow distributions and pressure losses for the combustion chamber of a commercial gas turbine aero engine. The need for such a model arose from practical problems being experienced on the particular gas turbine combustor considered. Results obtained showed that our simplified model is capable of predicting, with reasonable accuracy, the same trends as more detailed numerical models. The advantage, however, is the model's rapid execution, which allows design modifications and parametric studies to be conducted more simply than before. Moreover, the data obtained from the one-dimensional analysis were also used as boundary conditions for a more detailed three-dimensional model. The results were compared with the measured temperature distribution on the combustor outlet plane and overall good agreement was obtained.

Introduction

During the preliminary design phase of gas turbine combustors or when considering modifications to an existing design, it is essential to make realistic predictions of the mass flow splits through the various air admission holes, total pressure losses across the combustor as well as liner temperatures along the length of the combustor. The more accurate the initial design phase, the less time is spent on more advanced, three-dimensional simulations and rig tests, thus reducing development time and cost.¹⁻³

Traditionally, one-dimensional codes have been used during the preliminary design phase, although these are limited by the geometrical restrictive empirical correlations.⁴⁻⁶ Samuel³ described an analytical method that was based on the actual sequence of processes that the flow experiences as it passes

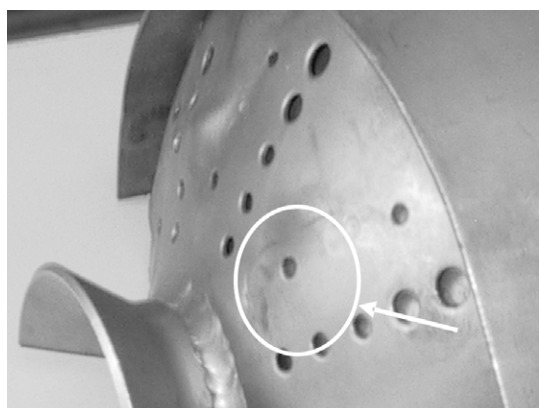
*Department of Mechanical and Aeronautical Engineering, University of Pretoria, Pretoria 0002, South Africa.

[†]Author for correspondence. E-mail: mmontres@up.ac.za

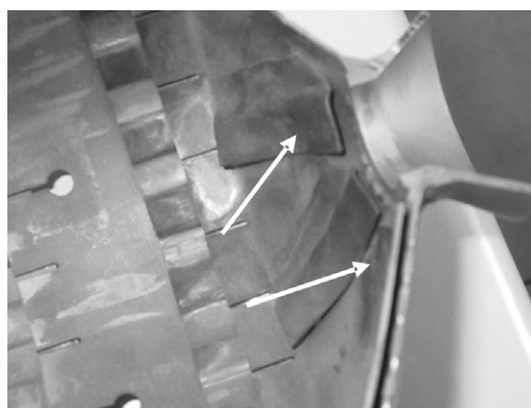
through the combustion system. The method calculated the pressure distribution and mass flow rates throughout a gas turbine combustor when inlet flow conditions and geometry of the system were known. Joubert and Hattingh⁷ described a similar approach in which the pressure drop and flow splits were calculated for a reverse-flow combustion chamber. The analysis employed the continuity, momentum, and energy conservation in a step-wise manner. The combustor model was divided into several stations and calculations proceeded from one station to the next by using the results from the previous station as input to the following one. Mongia *et al.*⁸ also used a one-dimensional model to predict mass flow distributions that could be used as boundary conditions for a three-dimensional model. However, the one-dimensional empirical approach is not that versatile and, when complex geometries need to be analysed, it is difficult to implement.

A network approach, on the other hand, is capable of modelling complicated geometries more effectively and rapidly. Stuttaford and Ribini⁸ described a network model consisting of independent sub-flows linked together to model a certain process, which can be described by overlaying a network on the system geometry comprising elements that are linked together by nodes. The elements define the actual geometrical features such as orifices and duct sections in the domain of interest. Semi-empirical formulations are used to describe the flow through the component elements, while the overall governing equations are solved within the nodes.^{9,10}

The purpose of the study described here was to develop a rapid one-dimensional model, by combining an empirical approach with a commercial network solver. Commercial network solvers, although capable of modelling a range of steady and transient incompressible and compressible flows, do not have the ability to model reactive flow as found in gas turbine combustors. The study therefore focused on the integration of the two different approaches to develop a model which allows several design modifications to be investigated on annular and can-annular gas turbine combustors, prior to involving more expensive three-dimensional models. Although the advantages of more expensive numerical models surpass simplified approaches, they remain time-consuming and computationally expensive. The need for such a model arose from crack formation problems experienced on a commercial combustor. These defects were believed to be due to high temperature gradients, which in some cases may even have been increased by blocked splash cooling strips on the dome (Fig. 1). The combustor design is rather old compared with modern-day systems but, because the



(a)



(b)

Fig. 1. Defects on combustor dome indicated by the arrows. (a) Crack formation on the dome section (circled); (b) thermal distortion of the splash cooling devices (arrowed) on the inside of the dome.

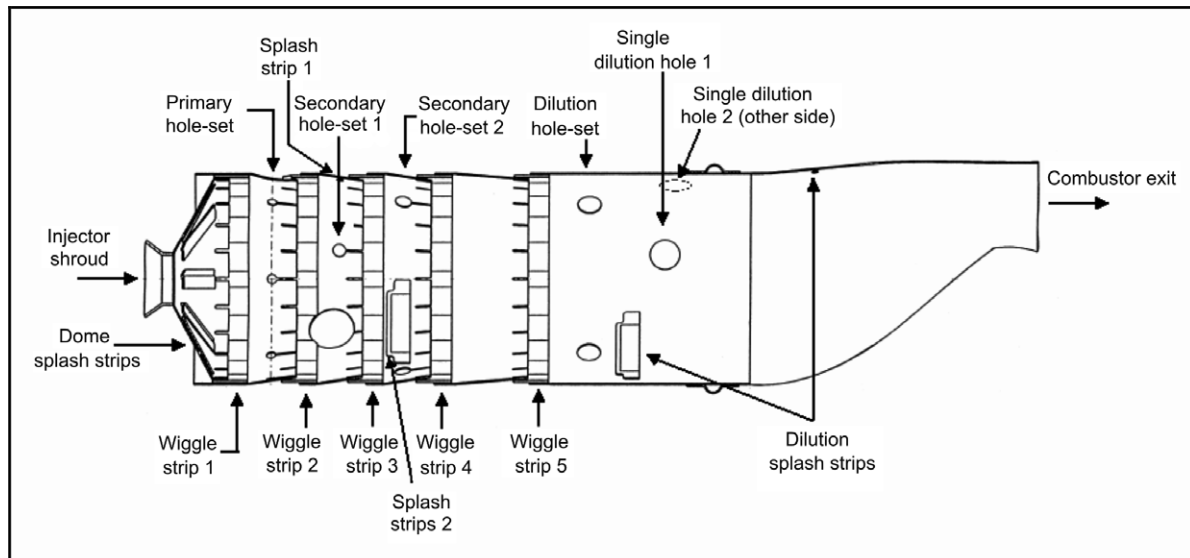


Fig. 2. Single combustion chamber and description of the combustor hole layout.

aircraft concerned is required to continue in operation for the foreseeable future, a need exists for improvement.

The combustion system investigated has a can-annular arrangement, consisting of six combustion liners positioned within an annular casing and exhaust into a four-stage turbine. A single combustor liner is depicted in Fig. 2. The primary zone contains a single hole-set comprising seven air admission holes. The secondary and dilution zones each consists of two hole-sets. The first and second hole-sets in the secondary zone comprise three and four holes, respectively, whereas the first and second hole-sets in the dilution zone comprise four and two holes, respectively. Use is made of eight splash strips on the dome to impart a swirling motion to the flow within the primary zone and to cool the dome wall. Film cooling air is admitted through five wiggle strip sets along the combustion liner as well as some splash cooling devices. Typical operating conditions during take-off and also used in this study are presented in Table 1.

Network model of the combustor

Initially, a one-dimensional empirical model was developed as part of the study.¹¹ The model employed an incompressible pressure drop–flow relationship through the individual hole types. The geometry is divided into four distinct zones: re-circulation, primary, secondary, and dilution zone. The total mass flow was then computed in each zone, after which the maximum temperature rise in each was determined from typical temperature rise curves for kerosene. Intermediate gas temperatures were calculated by interpolation between the zones followed by a heat balance in the radial direction to determine liner wall temperatures.

Although such an empirical code is not new, we chose to investigate the possibility of combining the empirical model with a commercial one-dimensional network solver. Network models employ conservation governing equations and are therefore suitable for both compressible and incompressible flow, while parameters such as gas temperatures, combustion efficiency, gas emissivity, and correlations to predict film cooling efficiencies can be obtained from the empirical formulations. By combining the two approaches rather than using only an empirical one, it is possible to obtain more detailed and realistic answers while still maintaining rapid execution time.

Figure A(a) (see supplementary material online) illustrates the network layout that was developed for the combustor under

Table 1. Operating conditions during take-off.

Combustor inlet temperature, T_{03} [K]	566
Combustor inlet pressure, P_{03} [Pa]	923 897
Total mass flow rate, m_a [kg/s]	14.154
Air–fuel ratio	50

consideration to solve the flow distribution through the different features without any heat transfer elements. Given its symmetry, only half of the combustor was modelled. The squares and circles, shown in more detail for the primary and secondary zone in Fig. A(b) (online), denote the nodes and elements, respectively. The type of element that was used varied depending upon the type of geometrical feature modelled. Inside the combustion chamber and annulus, DG elements (duct with variable area) were used. These elements account for area changes in a duct as well as frictional losses and momentum addition. The geometrical flow features, such as primary, secondary, and dilution holes, as well as film cooling devices were modelled with RD elements (restrictor with discharge coefficient). These elements are used when the combustor has a known discharge coefficient. A swirler, on the other hand, can be modelled with an RL element (restrictor with loss coefficient), which is similar to the RD element but accounts for the pressure drop through the feature contraction as well as accounting for loss coefficients.

The initial step in the computational scheme was to assume a pressure at all the nodes and to calculate the corresponding density. The flow rate could then be calculated from the initial pressure and density. Thereafter, a correction scheme, presented by Greyvenstein and Laurie,¹² was applied to the pressure, density, and flow rate to satisfy the governing equations. The overall governing equations constitute the continuity equation, which was applied at every node in the network, and the pressure drop–flow relationship, which was applied for every element. The pressure drop–flow relationship in each element is typically defined using the Darcy-Weisbach, Hazen-Williams, Manning or other exponential or empirically determined correlations.¹³ Mass and energy conservation was thus applied at the network nodes and momentum conservation was imposed across the elements.

Heat transfer was modelled with convective, radiative, and conductive heat transfer elements. The heat transfer process is

described between two nodes where enthalpy is balanced within each node, thereby satisfying the energy conservation equation. In the absence of a film cooling device, heat transfer from the combustion gases to the combustion liner was modelled with convective and radiative elements. These elements were connected to a conductive element which accounted for the conductive heat transfer through the combustor liner. External heat transfer was accounted for by the connection of a CHT (conductive heat transfer) element to the conductive element where, for simplicity, a constant convective heat transfer coefficient and radiation to the annulus air was specified. Axial conduction along the combustor liner was also incorporated into the model with a PCHT (primitive heat transfer) element. Such a process is illustrated in Fig. B (online) using only two heat transfer strings due to the complexity of the model, whereas several strings were actually used to obtain an adequate resolution. The black nodes denote nodes that have a fixed property assigned to them, in this case, a fixed temperature. Flame temperatures were predicted with the use of the empirical code using temperature rise curves¹⁴ and accounting for combustion efficiency in the various zones.

Radiation between the combustion gases and the combustor liner, and also between the liner and outer casings, were also considered. Radiation could not be modelled between the flow path and combustion liner due to the limitations of the network model. For this reason, an additional node with fixed temperature, similar to its flow path counterpart, was added to incorporate radiation from the combustion gases to the liner wall (Fig. B). The radiation element was connected between the additional node and the node connected to the CHT element, which describes conduction through the liner wall. Gas emissivities as well as heat transfer areas were defined within the radiation element. The gas emissivities were predicted as a function of flame temperature using semi-empirical correlations presented by Lefebvre.¹⁵

Modelling the effect of film cooling air on the combustor liner is generally done with the aid of empirical correlations, which make use of film cooling efficiency to predict the temperature increase of the film cooling air as it flows along the length of the combustor.^{16,17} Such correlations are, however, not available in the network model. A heat transfer process was therefore used from the hot combustion gases to the film cooling air in a series of heat transfer strings to model the temperature increase of the air as it flows further downstream from the point of injection. It was assumed that the film cooling air flowed from the point of injection up to the following geometrical feature. Figure C (online) illustrates the network layout used to define the flow and heat transfer process through a film cooling device. The latter was modelled with RD and DG elements to describe the flow through the cooling orifice and the flow path of the cooling air, respectively. For a specific film cooling heat transfer string, the film cooling air was heated through convection from the combustion gases – denoted by element 1 in Fig. C. The heat transfer of the film cooling air to the combustion liner was thereafter modelled with convection but with a heat transfer area similar to that of the cooling device. This process is depicted by element 2 in Fig. C. The remaining area that is not cooled by a film cooling device was heated by convection and radiation from the combustion gases, shown as elements 3 and 4 in Fig. C.

Network results

The incompressible empirical code was initially used to predict discharge coefficients (Cd) and jet angles using the correlations presented by Norster.¹⁷ The discharge coefficients were thereafter

defined as inputs to the network solver to predict flow distributions and pressure losses. However, the correlations presented by Norster¹⁶ are only valid for plain holes and not for cooling devices. Consequently, discharge coefficients had to be assumed for the cooling devices. According to Dodds and Bahr,¹⁸ if inadequate discharge coefficients are available for cooling devices, an appropriate initial guess is a value of 0.8. For the splash cooling devices a discharge coefficient of 0.6 was assumed.

Experimental isothermal flow distribution data were obtained from Van Niekerk and Morris¹⁹ for a single combustor liner at atmospheric operating conditions. Initially, these data were used to validate the predicted data obtained from the network solver. Table 2 (see supplementary material online) compares the experimental measurements with the initial predicted flow distributions obtained, as a fraction of the total mass flow rate. The predicted pressure loss obtained from the network solver is also shown. The data in Table 2 are described in sequence when moving from the dome, downstream towards the combustor exit as depicted in Fig. 2. The comparison between the predicted and experimental flow distribution data shows that there were discrepancies between the two sets of data. These discrepancies can be attributed mainly to the assumed discharge coefficients. More than 50% of the total inlet mass flow was distributed through the cooling devices, and consequently the pressure loss predictions and the flow distribution were sensitive to differences in the assumed coefficients.

Because the experimental flow distribution for the current combustor was known, however, it was possible to calibrate the network model to obtain more appropriate discharge coefficients. The calibration was done by systematically varying the coefficients in the network solver until the experimental flow distributions were obtained within an approximate error of 1%. Table 3 (online) presents the flow distributions and pressure loss predictions that were determined. Comparing the former pressure loss predictions in Table 2 with that in Table 3, it can be seen that the pressure loss almost doubled. The latter value is a more realistic pressure loss and this is an important parameter when considering design modifications, because it influences the overall efficiency of the engine. A comparison of the empirically determined discharge coefficients and those obtained from the calibration method is shown in Table 4 (online). It is evident that the largest discrepancies were between the cooling devices.

Numerical results

The data obtained from the one-dimensional analysis were used as boundary conditions for a more detailed three-dimensional model to assess the validity of the network results. A commercial finite volume code was used to solve the turbulent flow transport equations and appropriate physics. The k-epsilon model²⁰ with standard model constants provided turbulence closure to the Reynolds-Averaged Navier-Stokes equations²¹ with wall functions for the near-wall treatment. Combustion was modelled using the equilibrium mixture fraction model with an assumed β -probability density function, which is appropriate for the solution of turbulent diffusion flames with infinitely fast reactions.

The primary boundary conditions were the air and fuel inlets. The air inlet boundaries were prescribed with a uniform mass flow rate along with inlet temperature. The mass flow rates were obtained from the network results presented in Table 3 along with calculated jet angles. On the outlet plane, a pressure boundary condition was used. On the outside of the liner wall a constant heat transfer coefficient was prescribed, calculated from the average Reynolds number within the annulus. The fuel

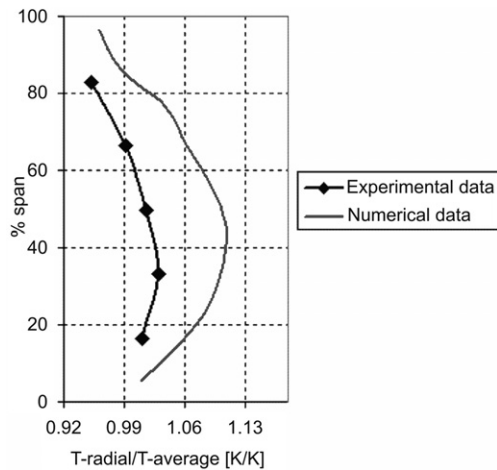


Fig. 3. Comparison of measured and predicted average exit temperature profiles on the combustor outlet plane.

distribution used in the numerical model corresponded with the experimental measurements obtained by Van Niekerk and Morris.¹⁹ The fuel spray was modelled as a discrete second phase and the droplets were tracked in a Lagrangian framework. The spray cone was modelled as 6 discrete cones covering the total included angle of 110° of the real spray. Radiation was modelled using the P-1 radiation model,²² which is a non-equilibrium diffusion type model, and the variation of the mixture's absorption coefficient was taken into account using the weighted-sum-of-Gray-gases model.²³

The accuracy of the numerical results was compared with the experimental measurements made by Skidmore (pers. comm.) on the outlet plane of the combustor. Temperature measurements were taken under the operating conditions specified in Table 1 and averaged on constant radii to obtain an averaged turbine inlet temperature (TIT) profile. The temperatures were then non-dimensionalized with the averaged measured temperature on the outlet plane. Figure 3 demonstrates the ability of the numerical model to predict the TIT profile. It can be seen that the profiles are similar, although the temperatures are over-predicted. The maximum predicted temperature was also obtained at a 40% span whereas the measured maximum was at a span of approximately 35%. However, overall differences in magnitude between the predicted and experimental data compared favourably and within 10% of each other. These differences can be attributed to the inaccuracies of the network model as well as to the limitations of the physical models employed in the numerical model. We also found that the highest temperatures were predicted on the dome section and transition piece. It is possible that these high temperatures and hence thermal gradients on the dome could be associated with the thermal distortion of the splash cooling devices shown in Fig. 1.

Conclusion

A one-dimensional incompressible empirical code was developed and coupled to a compressible network solver to predict flow distribution data and pressure losses across a combustion chamber in an aircraft engine. This method proved to be rapidly executed while still providing good results. Consequently, various design modifications can be investigated by this means, prior to invoking more detailed computational fluid dynamics analyses. The results obtained showed that discharge coefficients influenced the one-dimensional flow and pressure drop predictions significantly. Obtaining correlations for the prediction of discharge coefficients for any hole type is, however, a

difficult task. Hence, cold flow measurements were used to calibrate the simplified model to obtain correct discharge coefficients, flow distributions and overall pressure drop.

Furthermore, the results obtained from the analysis were used as boundary conditions for a more detailed three-dimensional numerical model incorporating the chemical reactions, turbulence and heat transfer. The mass flow distributions were used to calculate the jet angles that were prescribed at the various inlets. The fuel was modelled as a discrete secondary phase using a measured particle distribution. The results obtained from the numerical model were compared against measured average exit temperature profiles. Good agreement was obtained overall, with a maximum temperature difference of less than 10%. The numerical results also indicated higher temperatures to be present on the dome section, which corresponds with crack formation problems currently experienced with the combustor. Future work will include more detailed flow and temperature analyses to assess the influence of replacing the dome splash strips with an axial swirler.

1. Lawson R.J. (1993). Computational modelling of an aircraft engine combustor to achieve target exit temperature profiles. ASME Paper No. 93-GT-164.
2. Eccles N.C. and Priddin C.H. (1999). Accelerated combustion design using CFD. ISABE Paper No. 99-7094.
3. Samuel B.P. (1961). A jet engine combustor design analysis suitable for electronic computers. ASME Paper No. 61-WA-305.
4. McGuiirk J.J. and Spencer A. (2001). Coupled and uncoupled CFD predictions of the characteristics of jets from combustor air admission ports. *J. Engng Gas Turbine and Power* **123**, 327-332.
5. Hu T. and Prociw L.A. (1993). Recent CFD applications in small gas turbine combustion systems development. *Proc. 81st Symp. Propulsion and Energetic Panel on Fuel and Combustion Technology for Advanced Aircraft Engines*, AGARD Conference, Rome.
6. Mongia H.C. Reynolds R.S. and Srinivasan R. (1986). Multidimensional gas turbine combustor modelling: application and limitations. *AIAA J.* **24**, 890-904.
7. Joubert F.M. and Hattingh H.V. (1982). Rekenaar-modellering van 'n annulere teenvloei-verbrandingsruim vir gasturbinenjinns. *Journal of Aeronautical Society* **3**, 44-50.
8. Stuttaford P.J. and Rubini P.A. (1997). Preliminary gas turbine combustor design using a network approach. *J. Engng Gas Turbine and Power* **119**, 547-552.
9. Stuttaford P.J. and Rubini P.A. (1998). Assessment of a radiative heat transfer model for gas turbine combustor preliminary design. *J. Propulsion and Power* **14**, 66-73.
10. Stuttaford P.J. and Rubini P.A. (1996). Preliminary gas turbine combustor design using a network approach. ASME Paper No. 96-GT-135.
11. Gouws J.J. (2007). *Combining a one-dimensional empirical and network solver with computational fluid dynamics to investigate possible modifications to a commercial gas turbine combustor*. M.Eng. thesis, University of Pretoria, South Africa.
12. Greyvenstein G.P. and Laurie D.P. (1994). A segregated CFD approach to pipe network analysis. *International Journal for Numerical Methods in Engineering* **37**, 3685-3705.
13. White F.M. (1994). *Fluid Mechanics*, 3rd Edn. McGraw-Hill, New York.
14. Odgers J. and Kretschmer D. (1980). *The Design and Development of Gas Turbine Combustors*, vol. 2. Northern Research and Engineering Corporation, Woburn, Massachusetts.
15. Lefebvre A.H. (1998). *Gas Turbine Combustion*, 2nd edn. Taylor & Francis, London.
16. Stuttaford P.J. (1997). *Preliminary gas turbine combustor design using a network approach*. Ph.D. thesis, Cranfield University, Cranfield, U.K..
17. Norster E.R. (1980). *The Design and Development of Gas Turbine Combustors*, vol. 1. Northern Research and Engineering Corporation, Woburn, Massachusetts.
18. Dodds W.J. and Bahr D.W. (1990). Combustion system design. In *Design of Modern Gas Turbine Combustors*, ed. A.M. Mellor, pp. 343-476. Academic Press, San Diego.
19. Van Niekerk J.E. and Morris R.M. (2001). Prediction of T56 turbine inlet temperature profile with an abnormal fuel distribution. In *Proc. 17th International Symposium on Airbreathing Machines*, Munich, September 2005.
20. Launder B.E. and Spalding D.B. (1972). *Lectures in Mathematical Models of Turbulence*. Academic Press, London.
21. Versteeg H.K. and Malalasekera W. (1995). *An Introduction to Computational Fluid Dynamics*. Longman Scientific & Technical, New York.
22. Siegel R. and Howell J.R. (1992). *Thermal Radiation Heat Transfer*. Hemisphere Publishing, Washington, D.C.
23. Smith T.F. Shen Z.F. and Friedman J.N. (1982). Evaluation of coefficients for the weighted sum of gray gases model. *Journal of Heat Transfer* **104**, 602-608.

Supplementary material to:

Gouws J.J., Morris R.M. and Visser J.A. (2006). Modelling of a gas turbine combustor using a network solver. *S. Afr. J. Sci.* **102**, 533–536.

Table 2. Comparison of predicted and experimental flow distributions.

Hole type	Network predictions	Experimental	
	Mass fraction (%)	Mass fraction (%)	Error (%)
Injector shroud	0.7	–	–
Dome splash strips	4.63	6.14	24.6
Wiggle strip 1	12.74	15.63	18.4
Primary hole-set	3.01	4.82	37.5
Wiggle strip 2	12.75	10.69	–19.2
Secondary hole-set 1	2.26	3.51	35.7
Splash strip 1	0.87	0.19	–359.7
Wiggle strip 3	12.75	11.07	–15.1
Secondary hole-set 2	4.69	6.6	28.9
Splash strips 2	1.75	0.83	–110.5
Wiggle strip 4	12.75	9.59	–32.9
Wiggle strip 5	12.75	9.87	–29.1
Dilution hole-set	9.52	10.8	11.8
Dilution splash strips	2.62	2.62	–0.1
Single dilution hole 1	3.84	4.36	11.8
Single dilution hole 2	2.39	3.27	27.0
Pressure loss	2.24%		

Table 3. Comparison of calibration approach with experimental data.

Hole type	Calibration approach	Experimental	
	Mass fraction (%)	Mass fraction (%)	Error (%)
Injector shroud	0.74	–	–
Dome splash strips	6.09	6.14	0.81
Wiggle strip 1	15.51	15.63	0.79
Primary hole-set	4.78	4.82	0.82
Wiggle strip 2	10.61	10.69	0.72
Secondary hole-set 1	3.48	3.51	0.8
Splash strip 1	0.19	0.19	–0.17
Wiggle strip 3	10.99	11.07	0.68
Secondary hole-set 2	6.55	6.6	0.77
Splash strips 2	0.82	0.83	1.53
Wiggle strip 4	9.52	9.59	0.77
Wiggle strip 5	9.81	9.87	0.63
Dilution hole-set	10.73	10.8	0.69
Dilution splash strips	2.61	2.62	0.44
Single dilution hole 1	4.33	4.36	0.63
Single dilution hole 2	3.25	3.27	0.71
Pressure loss	5.10%		

Table 4. Comparison of predicted discharge coefficients.

Hole type	Assumed discharge coefficient	Calibration method discharge coefficient
Injector shroud	0.8	0.57
Dome splash strips	0.6	0.53
Wiggle strip 1	0.8	0.65
Primary hole-set	0.58	0.62
Wiggle strip 2	0.8	0.44
Secondary hole-set 1	0.58	0.60
Splash strip 1	0.6	0.087
Wiggle strip 3	0.8	0.46
Secondary hole-set 2	0.58	0.55
Splash strips 2	0.6	0.19
Wiggle strip 4	0.8	0.40
Wiggle strip 5	0.8	0.41
Dilution hole-set	0.58	0.44
Dilution splash strips	0.6	0.4
Single dilution hole 1	0.59	0.45
Single dilution hole 2	0.6	0.54

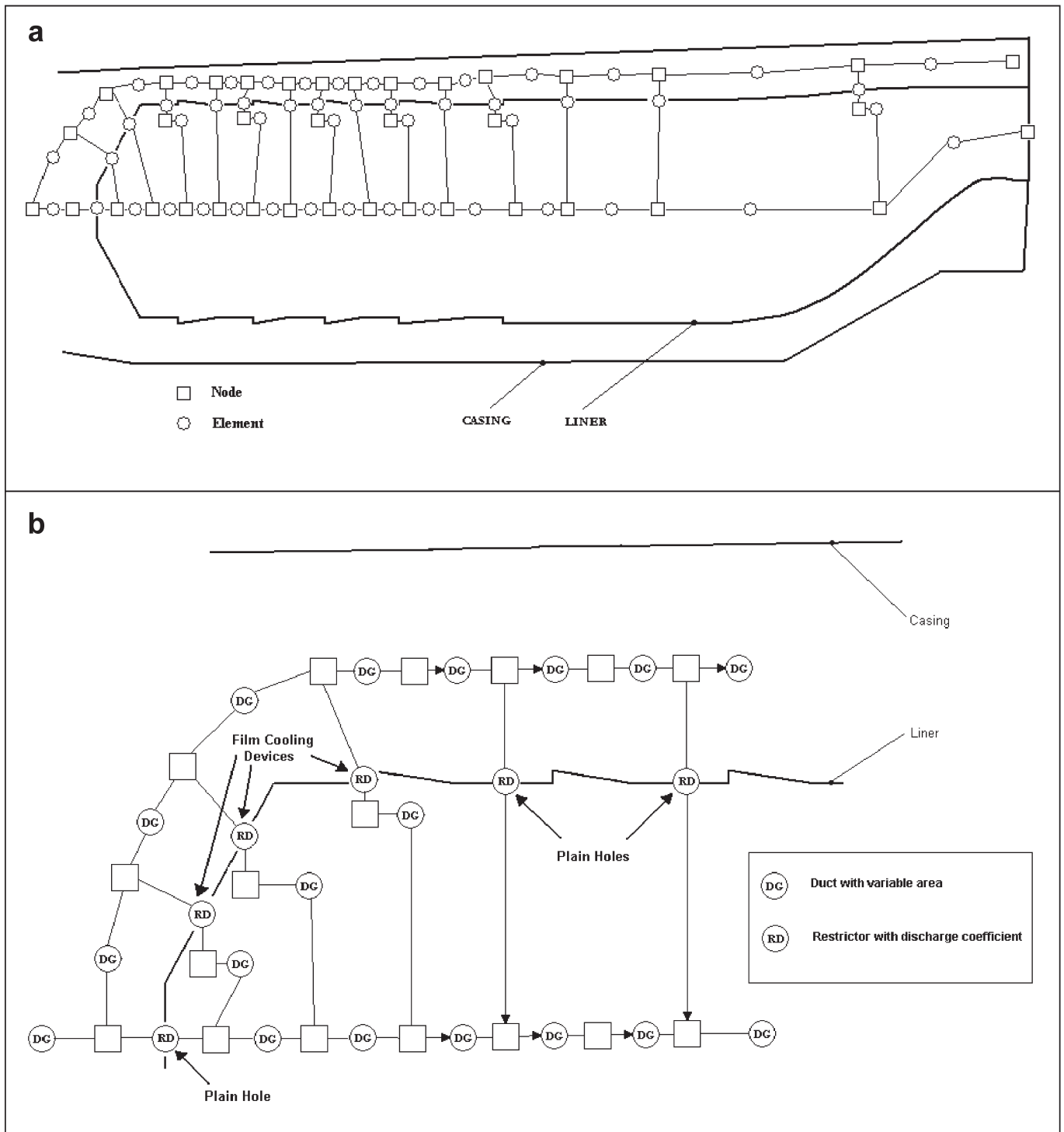


Fig. A. (a) General flow network layout for the combustion chamber; (b) primary and secondary zone network layout.

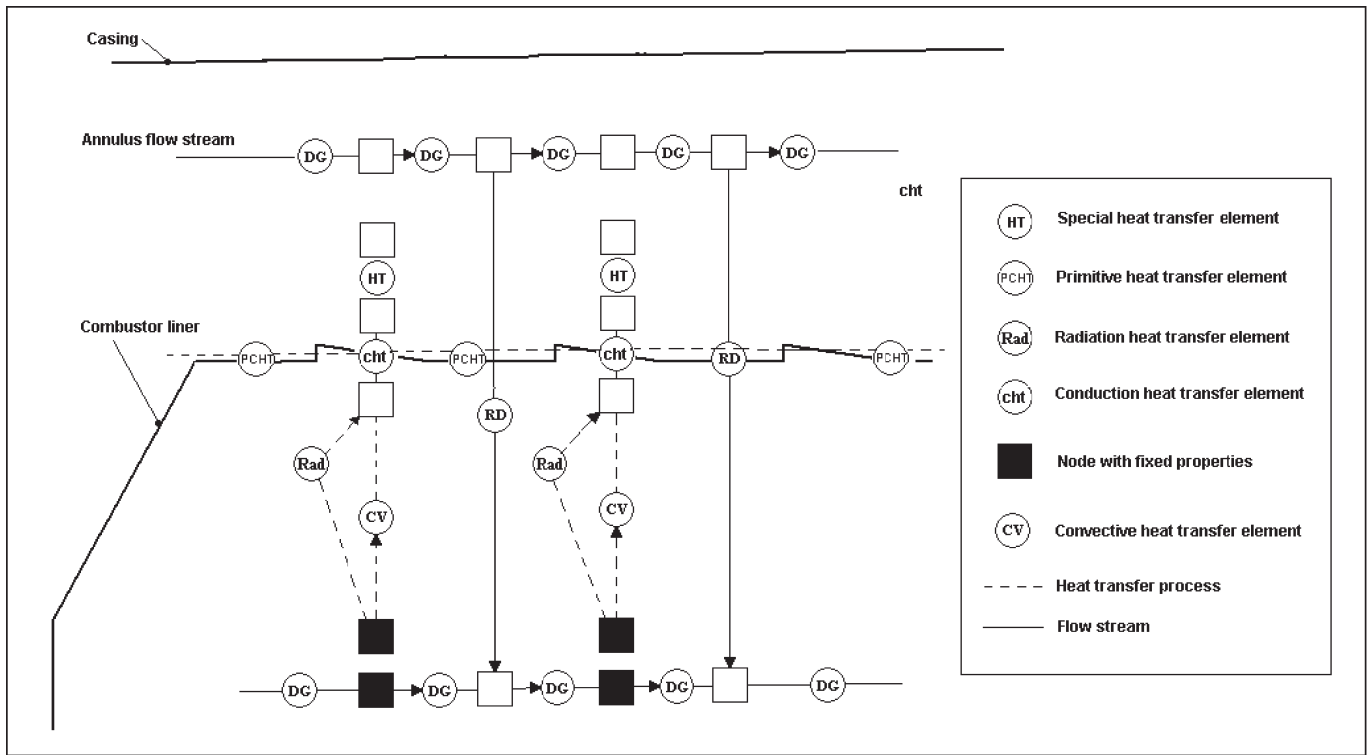


Fig. B. Heat transfer process network diagram without film cooling devices.

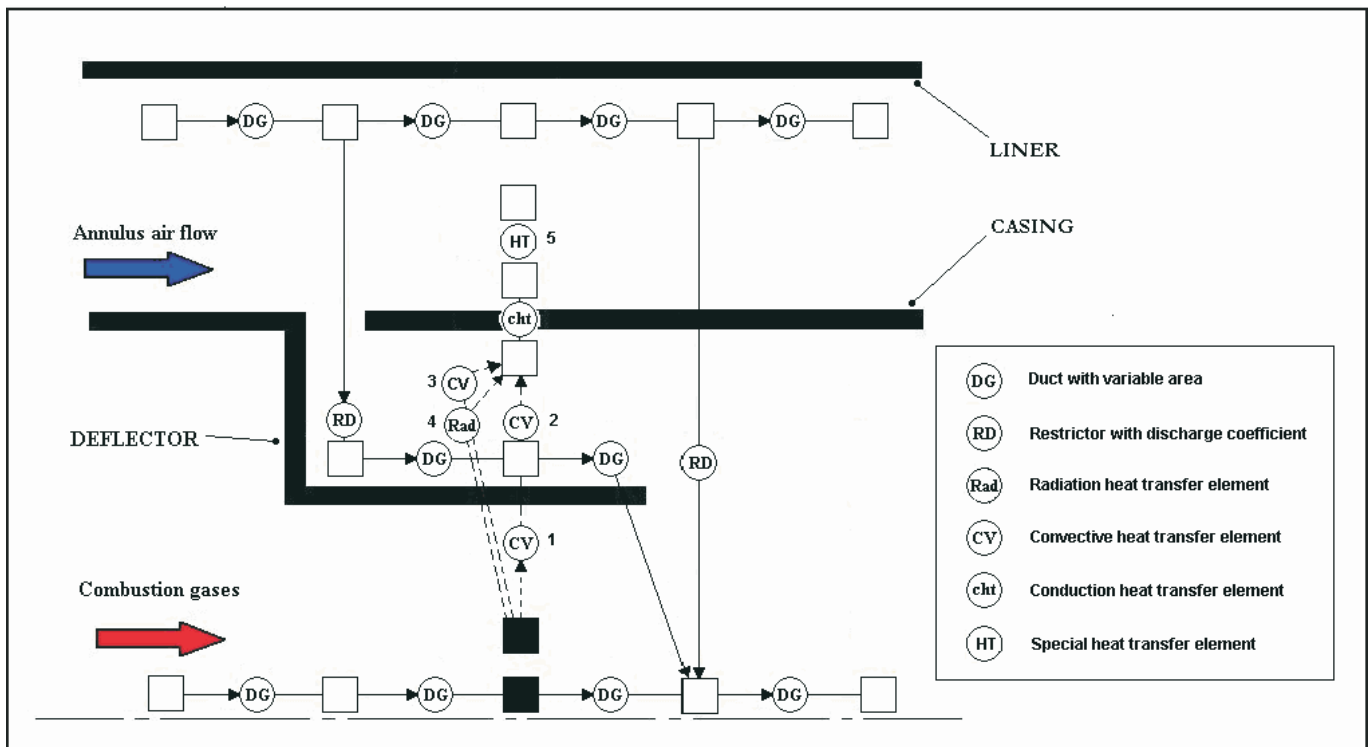


Fig. C. Heat transfer and flow layout for a film cooling device.